Journal of
Materials Chemistry C

Accepted Manuscript

This article can be cited before page numbers have been issued, to do this please use: Y. Fang, J. Hester, B. M. deGlee, C. Tuan, P. Brooke, T. Le, C. P. Wong, M. M. Tentzeris and K. H. Sandhage, *J. Mater. Chem. C*, 2016, DOI: 10.1039/C6TC01066K.

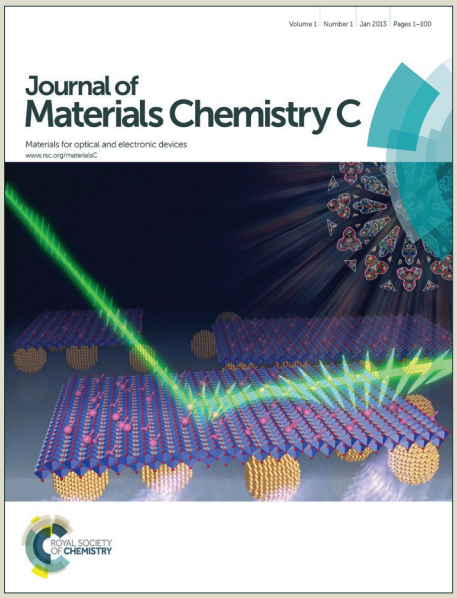




ROYAL SOCIETY OF CHEMISTRY

www.rsc.org/materialsC

View Article Online
DOI: 10.1039/C6TC01066K

Journal Name

ARTICLE

# A Novel, Facile, Layer-by-Layer Substrate Surface Modification for the Fabrication of All-Inkjet-Printed Flexible Electronic Devices on Kapton

Received 00th January 20xx,
Accepted 00th January 20xx

DOI: 10.1039/x0xx00000x

www.rsc.org/

Yunnan Fang,*[a] Jimmy G. D. Hester,[b] Ben M. deGlee,[a] Chia-Chi Tuan,[a] Philip D. Brooke,[a] Taoran Le,[b] Ching-ping Wong,[a] Manos M. Tentzeris,*[b] and Kenneth H. Sandhage*[ac]

A facile, environmentally-friendly, low-cost, and scalable deposition process has been developed and automated to apply polyelectrolyte multilayers (PEMs) on flexible Kapton HN substrates. Two weak polyelectrolytes, poly (acrylic acid) and polyethylenimine, were deposited in an alternating, layer-by-layer fashion under controlled pH and ionic strength. Compared to strong polyelectrolytes, weak electrolytes can control the properties of the PEMs more systmatically and simply. To our knowledge, this work on surface modification of Kapton is not only the first to use only weak polyelectrolytes, but is also the first to take advantage of the surface properties of calcium-bearing additive particles present in Kapton HN. The resulting surface-modified Kapton HN substrate allowed for the inkjet printing of water-based graphene oxide (GO) inks and organic solvent-based inks with good adhesion and with desired printability. While the deposition of a single PEM layer on a Kapton substrate significantly reduced the water contact angle and allowed for the inkjet-printing of GO inks, the deposition of additional PEM layers was required to maintain the adhesion during post-printing chemical treatments. As a conceptual demonstration of the general applicability of this PEM surface modification approach, a flexible, robust, single-layered gas sensor prototype was fully inkjet printed with both water- and ethanol-based inks and tested for its sensitivity to diethyl ethylphosphonate (DEEP), a simulant for G-series nerve agents. The electrical conductivity and morphology of the sensor were found to be insensitive to repeated bending around a 1 cm radius.

## 1. Introduction

Flexible electronics (such as electronic paper,[1,2] displays,[3] sensors,[4-6] photovoltaic cells,[7,8] electronic textiles,[9] LEDs,[10] electrochemical devices,[11] and RF tags[12]) are receiving increased attention by the scientific community and by industry because such flexibility, along with reduced weight and potentially lower cost, can enable new device applications relative to traditional rigid electronics. Among possible patterned deposition methods for high-throughput, high-volume and low-cost electronic devices, inkjet printing possesses an attractive combination of spatial resolution, printing speed, reproducibility, modest capital cost, and minimal waste. Furthermore, because inkjet-printing allows the designed device pattern to be directly applied to the substrate, dies, masks, chemical etchants, and complications associated with other patterning approaches are avoided.

Inkjet printing, often in combination with other deposition/patterning approaches (such as spin coating/patterning, screen printing/patterning, and plotter printing), has been used to fabricate numerous electronic devices (e.g., transistors,[13] light-emitting displays,[14] organic light-emitting diodes,[15] and solar cells[16]) on rigid hydrophilic substrates (e.g., silica-based glass, indium tin oxide (ITO) plates, *etc*.). The wetting of such rigid substrates by water and certain organic fluids used to dissolve/suspend ink particles has often been sufficient as to avoid the need for further surface modification to generate single-layered or multi-layered electronics. The hydrophobic or relatively inert nature of a number of common flexible polymeric substrates, however, complicates the process of inkjet printing with water-based solutions or suspensions. The desire to utilize such water-based inks for environmental and safety reasons provides a strong motivation for learning how to modify hydrophobic surfaces to allow for good printability of such inks. However, to allow for the complete inkjet printing of an entire device, the deposition of both water- and organic solvent-based inks on the same substrate surface may be required, which further complicates the surface functionalization and deposition processes.

Among the most commonly-used flexible substrates for inkjet-printing, Kapton films exhibit excellent flexibility, as well

[a] School of Materials Science and Engineering, Georgia Institute of Technology, Atlanta, GA 30332-0245, U.S.A. *Email: yunnan.fang@mse.gatech.edu
[b] School of Electrical and Computer Engineering, Georgia Institute of Technology, Atlanta, GA 30332-0250, U.S.A. *Email: etentze@ece.gatech.edu
[c] School of Materials Engineering, Purdue University, W. Lafayette, IN 47907-2045, U.S.A. *Email: sandhage@purdue.edu
† Electronic Supplementary Information (ESI) available. See
DOI: 10.1039/x0xx00000x

View Article Online
DOI: 10.1039/C6TC01066K



as thermal and chemical stability. Kapton films are comprised of a polyimide-based polymer which is hydrophobic and relatively inert. Accordingly, a number of methods, such as UV/ozone treatment,[17,18] plasma etching,[18,19] ion-beam etching,[20,21] acid[18,22] and/or base[23-25] treatments, and laser ablation,[26-28] have been used to modify polyimide to alter its inherent hydrophobicity. These methods use relatively harsh conditions to oxidize and/or remove part of the surface polyimide. As a result, the structural integrity and properties (such as the cohesive strength, and the thermal and chemical stability) of Kapton can be compromised by such treatments. Additionally, the by-products (such as the volatile hydrocarbon products from UV/ozone treatments) or wastes (such as strong bases and acids) generated from these harsh treatments are not environmentally friendly, which complicates the scale-up of such processes.

The application of polyelectrolyte multilayers (PEMs) on substrates, through the alternating deposition of oppositely-charged polyelectrolytes, can overcome the shortcomings of the aforementioned traditional harsh treatments. Prior work has demonstrated that the deposition of PEMs composed of strong polyelectrolytes can be tuned down to the molecular level (e.g., by adjusting the ionic strength of the solvent from which the polyelectrolytes are adsorbed). However, such control over the PEM thickness and composition can be relatively limited due to the poor solubility of polyelectrolytes in solutions of high ionic strength.[29] On the other hand, the properties (such as surface wettability, layer thickness, and layer interpenetration) of PEMs formed from weak polyelectrolytes can be systematically and simply controlled by varying their linear charge density via adjustment of the pH of the polyelectrolyte solutions.[29] To our knowledge, the gentle surface modification of Kapton substrates with the use of only weak polyelectrolytes, so as to enable the generation of crack-free inkjet-printed films on Kapton, has not been reported.

The aim of the present work has been to develop and demonstrate a facile, environmentally-friendly, gentle, low-cost, computer-automated, layer-by-layer (LbL) deposition process to apply PEMs to flexible Kapton HN films to allow for the deposition of flexible, inkjet-patterned electronic devices. In addition to the polyimide matrix, Kapton HN films contain a dispersion of calcium-bearing particles.[30] The LbL process was used to deposit alternating layers of two weak polyelectrolyte molecules of modest size under controlled ionic strength and pH values. Unlike the aforementioned surface modification methods, which used relatively harsh conditions targeted to affect the surface polyimide, our surface modification was conducted in mild aqueous solutions and was applied to the electrically charged surfaces of calcium-bearing additive particles. The effects of the PEM surface treatment: i) on the wetting of water, organic solvents, and inks, ii) on the deposition of crack-free graphene oxide (GO) films, and iii) on the adhesion of inkjet-printed GO films on Kapton HN substrates have been examined. To demonstrate the utility of the surface modification approach, a single-layered all-inkjet-printed flexible gas sensor prototype (composed of a reduced graphene oxide (rGO) patch and two silver electrodes) was fabricated with a water-based GO ink and an ethanol-based silver nanoparticle ink. The retention of the electrical performance of such a flexible sensor upon repeated bending was then examined. As a proof-of-concept demonstration, such a sensor was tested for its sensitivity to diethyl ethylphosphonate (DEEP), a simulant for G-series nerve agents.

## 2. Experimental procedure

### 2.1 Surface modification of Kapton HN substrates

A Kapton 500 HN sheet (a gift from Dupont, Wilmington, DE, USA) was cut into pieces with dimensions of 95 mm x 95 mm. These Kapton substrate pieces were cleaned by sonication first with a 10 g/L suspension of Powdered Precision Cleaner (Alconox, Inc., White Plains, NY, USA) in DI water for 10 min and then with acetone for 10 min in a 2510 Branson ultrasonic cleaner (Branson Ultrasonics, Danbury, CT, USA). After rinsing three times with DI water, the cleaned Kapton substrates were placed in the sample chamber of a custom-made, computer-controlled, automated deposition system. The substrates were then subjected to a layer-by-layer surface modification process which involved alternating exposure to solutions of oppositely-charged, relatively-small polyelectrolyte molecules, polyethylenimine (PEI) and poly (acrylic acid) (PAA). The electrostatic interaction of the PAA with PEI was used to generate the PEM layers (one PEM layer here refers to a layer of PAA plus a layer of PEI). The details of the automated surface modification process will be discussed in another publication. In brief, each of the polyelectrolyte solutions, and the 0.5 M NaCl rinse solution, used for the surface modification process was delivered to the sample chamber of the system with the aid of a peristaltic pump. After a given incubation step or rinsing step had been finished, the polyelectrolyte or rinse solution was removed from the sample chamber via a 2-way drain valve and captured in a waste chamber (i.e., the polyelectrolyte and rinse solutions were not re-used). The deposition parameters and process (i.e., the volume of each polyelectrolyte solution and the volume of the 0.5 M NaCl rinse solution delivered to the sample chamber, the order of incubation steps, and the time for each incubation step) were controlled by an appropriately programmed microprocessor which was used to operate the peristaltic pumps and the drain valve. In a typical deposition cycle, the Kapton substrates were incubated for 10 min in a 10 mg/ml PAA (average M.W. ~1,800 Dalton; Sigma-Aldrich, St. Louis, MO, USA) aqueous solution (pH adjusted to 5.1 with NaOH) containing 0.5 M NaCl. After rinsing three times with a 0.5 M NaCl aqueous solution, the Kapton substrates were then incubated for 10 min with a 10 mg/ml PEI (branched, M.W. 1,800 Dalton; Alfa Aesar, Ward Hill, MA, USA) aqueous solution (pH adjusted to 2.5 with HCl) containing 0.5 M NaCl. The substrate was then rinsed three times with 0.5 M NaCl aqueous solution. Such a PAA/rinse/PEI/rinse cycle was repeated to deposit the desired number of PEM layers on the substrates (note: the PEM coating was always terminated with

a final, external deposited layer of PEI). The surface-modified Kapton substrates were then rinsed with DI water, and dried in air at 60°C for 2 h.

As a test of the influence of electrostatic interactions with the Kapton HN surface, a control experiment was conducted in which the only modification of the deposition process was the use of an aqueous PAA solution with 1 M NaCl (instead of 0.5 M NaCl for the standard process).

Two traditional methods, UV/ozone treatment and plasma etching, were also used to modify the Kapton surfaces for control/benchmarking purposes. The UV/ozone treatment was conducted on 95 mm x 95 mm Kapton HN substrates using a UVO Cleaner (Jelight Company Inc., Irvine, CA, USA) for 5 min. Plasma etching was also conducted on such substrates using a plasma cleaner (model PDC-001. Harrick Scientific Corp., Ossining, NY, USA) in air for 20 min with the RF power set to the "High" level.

### 2.2 Ink formulation and inkjet printing

A water-based GO ink was prepared by adding an appropriate amount of glycerol (Amresco LLC, Solon, OH, USA) to a commercial GO solution (0.5 g/L, GO flake lateral dimensions = 0.3-0.7 µm, most flakes one atomic layer thick; Graphene Laboratories Inc., Calverton, NY, USA) to achieve a final glycerol concentration of 60 wt%, followed by vortexing to make a well-dispersed solution. The resulting GO ink was printed using an appropriate number (1-60) of passes on unmodified and surface-modified (UV/ozone treated, plasma etched, or PEM deposited) Kapton HN substrates. The inkjet-printed samples were then dried at 95°C under vacuum overnight to evaporate the water and glycerol.

A cyclohexanone/terpineol-based graphene ink was prepared based on the procedure of Secor *et al*.[31]

The silver patterns were inkjet-printed on the unmodified and PEM-modified Kapton substrates using 5 passes with a commercial silver nanoparticle ink (Sun Chemical Corporation, Parsippany, NJ, USA) followed by drying in air at 120°C for 3 h. All inkjet printing was conducted using a drop-on-demand piezoelectric inkjet printer (DMP-2800, Fujifilm Dimatix, Inc., Santa Clara, CA, USA).

### 2.3 Post-printing chemical treatments

To test the influence of various surface modification treatments (UV/ozone treatment, plasma treatment, and automated LbL PEM deposition) on film adhesion to Kapton HN substrates, inkjet-printed GO patch prototypes were prepared. The GO patch-bearing Kapton HN substrates were then subjected to a reduction process, in order to convert the electrically nonconductive GO to conductive rGO, followed by a series of water-, ethanol-, or dimethylformamide (DMF)-based chemical reactions. The purpose of the latter chemical treatments was to tailor the sensitivity and/or selectivity of all-inkjet-printed rGO-based gas sensors (to be discussed in a later publication).

Two types of reduction processes were examined to convert GO films into rGO: a dry thermal reduction treatment and a solution-based pyrrole reduction. The thermal reduction process was conducted at 300 °C for 1 h in nitrogen. The pyrrole reduction process was conducted using a reflux system at 100°C for 12 h in an aqueous solution containing 9 vol% pyrrole (98+% purity; Alfa Aesar, Ward Hill, MA, USA).[32] After pyrrole reduction, the resulting rGO-on-Kapton samples were washed first with water (3 times) and then with ethanol (2 times) followed by drying with flowing air at room temperature.

After reduction, the resulting rGO patches on Kapton HN were subjected to a series of water-, ethanol-, or DMF-based solutions to introduce various surface chemical functional groups to the patches. The details of such chemical functionalization treatments will be described in a later publication. In brief, these treatments were used to apply amine, acrylate, and hydroxyl groups to the surface of the rGO patches. Some of the rGO/Kapton HN specimens were functionalized with hexafluroisopropyl groups immediately after the reduction process.

### 2.4. Gas sensing

Gas sensing was performed with a home-made automated sensing system. The vapor stream (2.0 ppm) of diethyl ethylphosphonate (DEEP) was generated from a DEEP permeation tube (KIN-TEK Laboratories, Inc., La Marque, TX, USA) in a FlexStream™ Gas Standards Generator (KIN-TEK Laboratories, Inc.) and carried by nitrogen with a flow rate of 500 SCCM.

### 2.5 Materials Characterization

Lyophilization was performed using a Labconco Freezone® 18 freeze dryer (Labconco, Kansas City, Mo, USA). Scanned images were obtained from an Epson Perfection V370 Photo scanner. Scanning electron microscopy (SEM) was conducted with a field emission scanning electron microscope (Leo 1530 FEG SEM, Carl Zeiss SMT Ltd., Cambridge, UK) equipped with an energy dispersive X-ray spectrometer (INCA EDS, Oxford Instruments, Bucks, UK). X-ray diffraction (XRD) analyses were conducted with Cu Kα radiation using an X-Pert Pro Alpha-1 diffractometer equipped with an incident beam Johannsen monochromator and an Xcelerator linear detector (PANalytical). Contact angle measurements were conducted on a Rame-Hart goniometer equipped with a CCD camera (Rame-Hart Instrument Co., Succasunna, NJ, USA). Atomic force microscopy (AFM) was conducted with a Veeco Dimension 3100 Scanning Probe Microscope (Veeco Instruments, Inc., Plainview, NY, USA). The electrical resistance was measured on an Agilent 34401A 6 ½ Digit Multimeter (Agilent Technologies, Santa Clara, CA, USA).

## 3. Results and discussion

### 3.1 Roughness measurements

Atomic force microscopic (AFM) analyses were performed to determine the surface roughness of the unmodified and the PEM-modified Kapton HN substrates. The roughness values of

unmodified Kapton, and of Kapton treated with 1, 3 and 4 layers of PEMs, are shown in Table 1.

The values of both arithmetic (Ra) and quadratic (Rq) mean surface roughness increased slowly as the number of deposited PEM layers increased on the Kapton substrates. The AFM data (Table 1) indicated that the rate of increase in roughness with an increasing number of PEM layers was quite modest, which may be due to the small size of the polyelectrolytes (both PEI and PAA used in this work had a relatively low molecular weight of about 1,800 Daltons) and to the high ionic strength in the polyelectrolyte solutions; that is, the small size and high ionic strength could act to effectively reduce the dangling of tail or loop components of the polyelectrolyte molecules in the solution after adsorption onto the substrate.[33] Because the surface roughness of the resulting Kapton HN substrate increased only by a few nm (Ra from 0.67 to 1.76 nm and Rq from 0.89 to 2.59 nm) after four full cycles of PEM deposition (Table 1, Fig. 1), the effect of this roughness increase on the printing quality and on the surface roughness of the resulting inkjet-printed films was considered negligible.

### 3.2 Contact angle measurements

Contact angle measurements were conducted to evaluate the wetting of water, organic solvents, and inkjet inks on unmodified and PEM-modified Kapton substrates. As shown in Table 2, the contact angles of water and the water-based GO ink (which contained 60 wt% of glycerol to adjust the viscosity from 0.9 cP to 10 cP for inkjet printing) on unmodified Kapton HN were relatively large (76.6° and 72.4°, respectively).

On the other hand, the contact angles for the organic solvents (ethanol and DMF) on unmodified Kapton HN substrates were quite small (<13°). The commercial ethanol based-silver ink exhibited an average contact angle of 25.2°, which was slightly higher than those of the two organic solvents. The pure ethanol and the commercial ethanol-based silver ink possessed viscosities of ~1.0 cP and ~10 cP, respectively. The likely presence of one or more viscosity modifiers in the silver ink may have be responsible for the higher contact angles observed for such commercial silver inks on unmodified and PEM-modified Kapton HN substrates relative to pure ethanol.

PEM deposition on the Kapton HN substrates resulted in a significant and reproducible reduction in the contact angle exhibited by water and the water-based GO ink relative to unmodified substrates. After the deposition of only one layer of PEM on Kapton HN, the average contact angles of water and the water-based GO ink decreased to 41.0° and 55.5°, respectively, whereas little change was detected in the contact angles exhibited by the organic solvents (ethanol and DMF) and by the organic solvent-based silver ink after this treatment (Table 2). Deposition of additional PEM layers still resulted in negligible changes in contact angles for ethanol, DMF and the ethanol-based silver ink (Table 2). The relative insensitivity of the contact angles exhibited by ethanol, DMF, and the ethanol-based silver ink to the PEM-modification of the Kapton surface may be due to the polar nature of both ethanol and DMF, which could allow for attraction of these solvents to charged, PEM-modified Kapton HN surfaces. The deposition of additional PEM layers on the Kapton substrates resulted in little further change in the observed contact angles for all solvents and inks examined in this work (i.e., water, ethanol, DMF, water-based GO ink, and ethanol-based silver ink), which was consistent with previous observations that the wetting of fluids onto sequentially-adsorbed polyelectrolyte layers was affected primarily by the outermost/surface layer.[32,33]

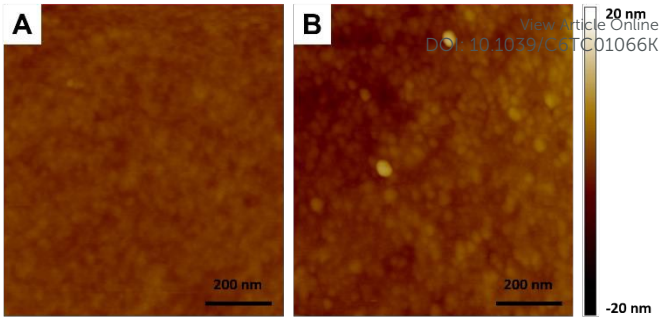


**Fig. 1.** A) AFM images of unmodified Kapton HN and B) Kapton HN after deposition of 4 PEM layers.

### 3.3 Printability assessment

As the next step for the evaluation of the Kapton surface modification process, two organic solvent-based inks (an ethanol-based silver ink and a cyclohexanone/terpineol-based graphene ink) and a water-based GO ink were examined for their inkjet printability on Kapton HN substrates before and after PEM deposition. Taking advantage of the thin film nature of both the inkjet-printed patterns (silver IDEs and graphene patches) and the Kapton substrates, the silver IDE and graphene patterns inkjet-printed on various Kapton HN substrates were scanned with a high-resolution scanner to show the printing qualities. Due to the strong color contrast between the silver IDEs (silver grey) and the Kapton HN

**Table 1**. Roughness (arithmetic mean surface roughness, Ra; quadratic mean surface roughness, Rq) of unmodified and PEM-modified Kapton HN substrates.

| | Unmodified Kapton | Kapton with 1 PEM layer | Kapton with 3 PEM layers | Kapton with 4 PEM layers |
|---|---|---|---|---|
| Ra (nm) | 0.67 ± 0.07 | 0.82 ± 0.59 | 1.40 ± 0.41 | 1.76 ± 0.33 |
| Rq (nm) | 0.89 ± 0.13 | 0.80 ± 0.14 | 2.08 ± 0.77 | 2.59 ± 0.48 |

**Table 2**. Contact angles of different fluids/inks on unmodified and PEM-modified Kapton HN substrates.

| | Unmodified Kapton | Kapton with 1 PEM layer | Kapton with 3 PEM layers | Kapton with 4 PEM layers |
|---|---|---|---|---|
| Water | 76.6 ± 3.9 | 41.0 ± 2.4 | 39.8 ± 1.9 | 37.4 ± 1.2 |
| Ethanol | 10.4 ± 2.5 | 12.1 ± 1.4 | 10.4 ± 1.9 | 12.2 ± 4.8 |
| DMF | 11.5 ± 1.3 | 12.5 ± 1.5 | 12.9 ± 0.1 | 13.3 ± 2.6 |
| Water-based GO ink | 72.4 ± 3.5 | 55.5 ± 2.6 | 53.7 ± 1.9 | 51.5 ± 1.2 |
| Ethanol-based silver ink | 25.2 ± 1.8 | 23.6 ± 0.3 | 24.1 ± 1.1 | 26.4 ± 1.6 |

View Article Online
DOI: 10.1039/C6TC01066K





(reddish brown) and between the graphene patches (black) and Kapton HN, printing defects can be easily spotted in the scanned high magnification images. For example, Fig. S1 shows scanned images of a silver IDE pattern (Fig. S1A) and a graphene patch (Fig. S1B) inkjet-printed on surface unmodified Kapton HN films using an ethanol-based silver ink and a cyclohexanone/terpineol-based graphene ink, respectively, with the graphene and silver traces intentionally damaged. The defects caused by the intentional damage can be easily identified by the reddish brown color from the uncovered or thinly-covered Kapton HN substrate. Figs. S2 and S3 reveal scanned images of silver IDE patterns and graphene patches, respectively, inkjet-printed on unmodified Kapton HN and Kapton HN which had been deposited with 1, 3 and 4 layers of PEMs with the same organic solvent-based inks as those used for Fig. S1. All of the silver and graphene patterns shown in Figs. S2 and S3 appeared morphologically uniform with precisely-controlled shapes and sharp edges, as designed, regardless of whether they were printed on surface modified or unmodified Kapton HN substrates.

The water-based GO ink was then inkjet printed on both unmodified and PEM-modified Kapton substrates. As revealed in Fig. 2A, the GO ink that was printed (5 passes) on an unmodified Kapton substrate tended to ball up to form isolated small "islands", which would result in a noncontinuous and nonuniform GO film after the drying of the ink. However, with a Kapton substrate that had been surface modified with 1, 3 or 4 PEM layers, precisely-controlled liquid squares with sharp edges could be inkjet-printed, as designed. Fig. 2B shows a typical square pattern printed with the water-based GO ink on a Kapton substrate that had been surface modified with 4 PEM layers. The inkjet-printed GO square on the PEM-modified Kapton substrate (i.e., the specimen shown in Fig. 2B) was dried at 95°C under vacuum overnight, to allow for evaporation of the water and glycerol. Secondary electron images of the dried film are shown in Figs. 2C (low magnification) and 2D (high magnification). The dried GO square had sharp edges as designed and the GO flakes were well interconnected with no observable microcracks in the GO film. The dried films also did not exhibit an apparent "coffee ring" effect, which commonly occurs during the drying of printed aqueous ink suspensions. The coffee ring effect results in the deposition of an appreciable amount of solid ink material at the film perimeter upon ink drying (due to capillary-driven fluid flow during drying). The apparent absence of such an effect in the dried GO films printed onto the PEM-modified Kapton HN substrate suggests that local electrostatic interactions between the positively-charged surface-modified Kapton HN substrate (note: the surface-modified Kapton HN substrates were terminated with positively-charged PEI) and the negatively-charged GO flakes may have inhibited the migration of the GO flakes to the film perimeter during drying.

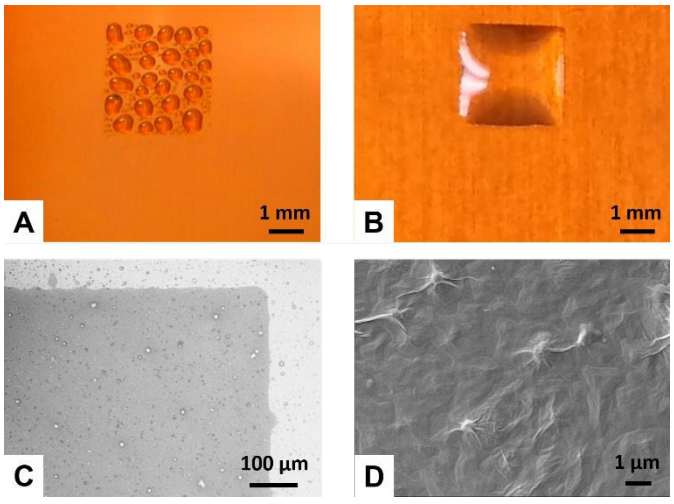


**Fig. 2.** Optical and secondary electron (SE) images of GO patterns printed (5 passes) with a water-based GO ink on unmodified and PEM-modified (with 4 PEMs) Kapton substrates. A) Optical image of a GO pattern printed on an unmodified Kapton substrate. B) Optical image of a GO pattern printed on a PEM-modified (with 4 PEM layers) Kapton substrate. C), D) SE images with low (C) and high (D) magnification of the specimen shown in B) after drying and removal of glycerol.

In order for negatively-charged PAA to bind electrostatically to Kapton HN substrates during the initial deposition step of the PEM-coating process, the Kapton HN substrate should be positively charged. X-ray diffraction (XRD) analysis of a PEM-modified (4 PEM layer) Kapton HN substrate is shown in Fig. 3a. The sharp diffraction peaks (labelled with filled diamonds) in Fig. 3a were consistent with the reference pattern for calcium carbonate, $CaCO_3$ (ICDD reference code 04-001-7249). (Note: it has previously been suggested that Kapton HN films contained dispersed particles of calcium phosphate dibasic, $CaHPO_4$.[34] However, the XRD pattern in Fig. 3a did not match any of the $CaHPO_4$ patterns in the PDF-4+2014 database or Crystallography Open Database, COD. While amorphous $CaHPO_4$ or a small amount of crystalline $CaHPO_4$ may be present, our XRD data indicates the presence of an appreciable amount of crystalline $CaCO_3$ in the Kapton HN films.) Calcium carbonate possesses an isoelectric point of 8.2.[35] Under the conditions of our surface modification treatment, $CaCO_3$ particles on the Kapton HN surface should be positively charged and, hence, could enable electrostatic binding of the initial PAA layer.

To evaluate the role of positive surface charges on the Kapton HN surface on the LbL electrostatic deposition process, the process was modified by using aqueous PAA solutions with

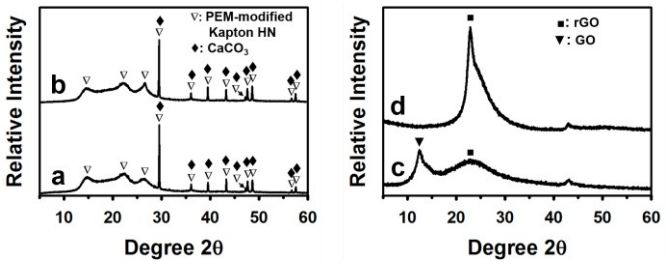


**Fig. 3.** XRD analyses of: a) a PEM-modified (4 PEM layers) Kapton substrate, b) GO printed on a PEM-modified (4 PEM layers) Kapton substrate after thermal reduction, c) GO powder obtained from lyophilized GO ink, and d) rGO powder after drying and thermal reduction of GO ink.

a higher NaCl concentration (i.e., 1 M NaCl instead of 0.5 M NaCl). We assumed that, in the presence of a higher concentration of NaCl, the positive charges on the surface of the $CaCO_3$ particles in Kapton HN would be more effectively screened by the $Cl^-$ ions. Hence, the electrostatic interaction between the PAA and the Kapton HN surface would be reduced, with a corresponding reduction in the extent of PAA binding to Kapton surface. After deposition of 4 PEM layers on the Kapton HN surface with the modified LbL PAA/PEI process using the PAA solution containing 1 M NaCl, inkjet printing was used to apply an aqueous GO solution (in a similar manner as conducted above). The resulting wet film balled up and formed isolated small "islands" (Fig. S4), similar to the patterns printed on an unmodified Kapton substrate (Fig. 2A). Hence, this control experiment indicated the importance of the presence of unscreened positive charges on the Kapton HN surface to allow for a uniform and high loading of the PAA/PEI multilayers.

### 3.4 Adhesion sustainability tests after chemical treatments

In order to enhance the sensitivity and/or selectivity of an inkjet-printed sensor, chemical treatments (such as reduction/oxidation and the introduction and/or amplification of particular chemical functional groups on the film surface) are usually conducted on printed GO sensor materials. The adhesion between the inkjet-printed GO sensing material and the substrate must be able to survive such chemical treatments.

To evaluate the relative adhesion of inkjet-printed GO-based sensors after such chemical treatments, the water-based GO-bearing solution was first inkjet-printed onto Kapton HN substrates that had been surface modified via 3 treatments: i) UV/ozone exposure, ii) plasma exposure, and iii) the standard LbL PEM deposition process described above. Either thermal (dry) or pyrrole (liquid-based) reduction was then conducted to reduce the inkjet-printed GO into rGO, followed by chemical treatments to introduce various surface chemical functional groups (hexafluroisopropyl, amine, acrylate, and hydroxyl groups) to the resulting rGO patches. In order to determine if either of the reduction methods was able to reduce the GO in inkjet-printed films into rGO, XRD analyses were used to evaluate the phase content of the films before and after either reduction process. Fig. 3b reveals the diffraction pattern obtained from the GO film after the thermal reduction process. This diffraction pattern was essentially the same as for the PEM-modified Kapton HN substrate that was not coated with GO (Fig. 3a); that is, XRD analysis of the coated Kapton HN was unable to differentiate the presence of GO or rGO in the thin film. Unfortunately, the highest intensity XRD peaks of both GO (located at a 2θ of ~12.0°[36]) and rGO (located at a 2θ of ~22.0°[36]) overlapped with the broad peak (from ~10° to ~35°) associated with the polyimide within the Kapton HN substrate.

A second approach was then examined for evaluating the efficacy of the aforementioned reduction methods. An appropriate amount of GO ink solution was dried under the same conditions as used to dry the inkjet-printed GO films (i.e., dried at 95°C under vacuum overnight), followed by one of the two reduction processes. The commercial GO solution used to prepare the GO ink was also lyophilized and the resulting dry particles were then subjected to XRD analyses. As revealed by the XRD pattern in Fig. 3c, the starting GO particles contained a small amount of rGO (as revealed by a modest broad diffraction peak located at a 2θ value of ~22.9°[36]). The XRD pattern shown in Fig. 3d indicates that the thermal reduction process conducted on the dried GO ink resulted in an increase in the rGO content, and a reduction in the GO content, of the ink. The XRD pattern obtained from the pyrrole-reduced sample was similar to that shown in Fig. 3d (Fig. S5), which indicated that both reduction methods were successful in converting GO into rGO.

After a given reduction or GO film functionalization process (to introduce certain functional groups to the inkjet-printed films), the adhesion between the inkjet-printed GO and the surface-modified Kapton substrate was visually inspected while slowly bending the rGO-on-Kapton structure to a radius of curvature of ~1 cm. The film was first bent 150 times in tension and then another 150 times in compression. The results of such adhesion sustainability bend tests on inkjet-printed GO films on surface-modified Kapton substrates, after exposure to a reduction process and a series of other chemical treatments, are summarized in Table 3 (in which GO was reduced to rGO by dry thermal reduction) and Table 4 (in which GO was reduced to rGO by the liquid pyrrole reduction method). The inkjet-printed GO films deposited on all of the surface-modified Kapton HN substrates that were then exposed to the dry thermal reduction step remained attached to the substrates after such bending. The GO films deposited on the 3-PEM-layer-modified or 4-PEM-layer-modified Kapton HN substrate, that were thermally reduced and then exposed to each of the film functionalization treatments, remained attached upon bending (Table 3). The adhesion of GO films deposited on the UV/ozone, plasma-modified, or 1-PEM-layer-modified Kapton HN substrates, followed by thermal reduction, was not as universally robust after the various film functionalization treatments. Table 4 reveals that only the GO films deposited on the 3-PEM-layer-modified and 4-PEM-layer-modified Kapton HN substrates, followed by pyrrole reduction, remained attached to the substrates after bending. Only the GO films deposited on the 4-PEM-layer-modified Kapton HN substrates, followed by pyrrole reduction and each of the film functionalization treatments, remained attached to the substrate after bending. It can be concluded from Tables 3 and 4 that the adhesion sustainability increased with increasing number of PEM layers deposited on the Kapton substrates. This is probably due to the following reasons: During the layer-by-layer PEM deposition process, every time after a polyelectrolyte (polyanion or polycation) was absorbed to the surface of blank Kapton HN surface or the oppositely charged polyelectrolyte which had been previously absorbed, there were still nonoccupied binding places (point charges) on the surface.[33] As a result, deposition of only one PEM layer would probably be able to cover most (which allows for reasonably

 

**Table 3**. Adhesion sustainability (as determined from bend tests) of GO films on surface-modified Kapton HN films upon thermal reduction and then a series of surface group-introducing reactions.

| Modification to GO \ Modification to Kapton | UV/ ozone* | Plasma | 1 PEM layer | 3 PEM layers | 4 PEM layers |
|---|---|---|---|---|---|
| Thermal reduction | + | + | + | + | + |
| Hexafluroisopropyl addition | - | - | + | + | + |
| Amine addition | - | - | + | + | + |
| Acrylate addition | NA | NA | - | + | + |
| Hydroxyl addition | NA | NA | NA | + | + |

*A positive sign "+" means the adhesion between the GO film the surface-modified Kapton HN substrate survived the corresponding chemical treatment, while a negative sign "-" means it did not. "NA" means the chemical treatment was not performed since the GO film had been peeled away from the substrate during a prior step.

good printability for water-based inkjet inks), but not all, of the blank Kapton HN surface with PEMs. As the deposited PEM layers increased, the uncovered surface of Kapton HN substrate gradually decreased and the positive charge density on the substrate gradually increased and, as a result, when the negatively charged GO ink particles were inkjet-printed on and bound to (via electrostatic interaction) such surface modified substrate, the strength of the adhesion between the inkjet-printed film and the substrate gradually increased."

Apparently the adhesion of the GO films was degraded to a greater degree by the pyrrole reduction process than the thermal reduction process. In any event, since the GO-coated, 4-PEM-layer-modified Kapton HN samples survived all of the reduction and film functionalization processes, this layer-by-layer surface modification approach was then used to generate all-inkjet-printed sensors.

### 3.5 Fabrication and bend testing of all-inkjet-printed flexible gas sensors

To demonstrate the utility of the PEM-modification approach used in this work, a single-layered, all-inkjet-printed gas sensor was fabricated on a PEM-modified Kapton HN substrate. Briefly, a GO patch was inkjet-printed with the water-based GO ink (Fig. 4, Step 1). After evaporation of water and glycerol, the thermal reduction process was used to convert the GO in the film into rGO (Fig. 4, Step 2). Two silver electrodes were then

**Table 4**. Adhesion sustainability of GO films on surface modified Kapton films upon pyrrole reduction followed by a series of surface group-introducing reactions.

| Modification to GO \ Modification to Kapton | UV/ ozone | Plasma | 1 PEM layer | 3 PEM layers | 4 PEM layers |
|---|---|---|---|---|---|
| Pyrrole reduction | - | - | - | + | + |
| Hexafluroisopropyl introduction | NA | NA | NA | + | + |
| Amine introduction | NA | NA | NA | + | + |
| Acrylate introduction | NA | NA | NA | - | + |
| Hydroxyl introduction | NA | NA | NA | NA | + |

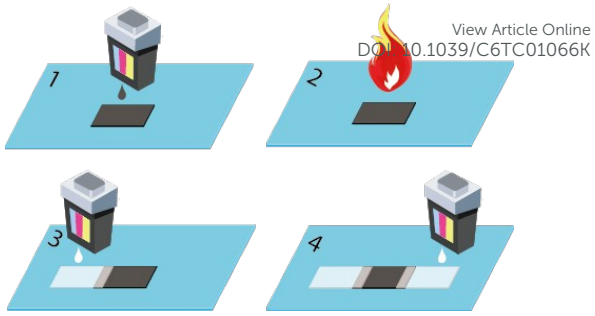

**Fig. 4.** Process for generating an all-inkjet-printed gas sensor on a PEM-modified flexible Kapton substrate with both water- and organic solvent-based inks. Step 1: Inkjet-printing of a GO film with a water-based GO ink. Step 2: Thermal reduction of the GO into rGO. Step 3: Inkjet-printing of one silver electrode with the ethanol-based silver nanoparticle ink. Step 4: Inkjet-printing of another silver electrode with the silver nanoparticle ink.

applied, via inkjet printing with the ethanol-based silver nanoparticle suspension, onto the Kapton HN substrate, with both electrodes overlapping the rGO patch by 1.5 mm for optimum contact between the rGO patch and the silver electrodes (Fig. 4, Steps 3 and 4). Finally, the resulting Ag-rGO-Kapton film assembly was heated in air at 120°C for 3 h to allow for the removal of the organic materials present on the silver nanoparticles and to allow for enhanced bonding of the silver nanoparticles to each other. Fig. 5A reveals an optical image of such a single-layered, all-inkjet-printed gas sensor fabricated following the steps illustrated in Fig. 4 on a Kapton substrate that had been coated with 4 PEM layers. The GO suspension was printed using 60 inkjet passes and the silver ink was printed using 5 passes for each electrode. The conductivity measurement with a multimeter showed that the

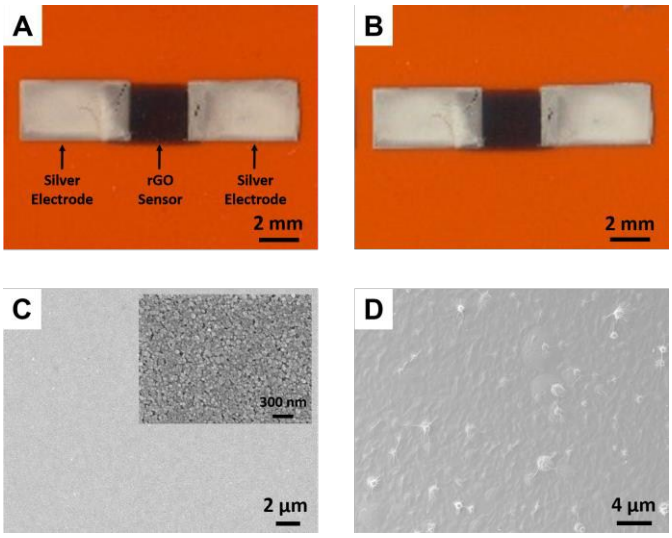


**Fig. 5.** Optical and secondary electron (SE) images of a single-layered, all-inkjet-printed rGO sensor printed on a PEM-modified Kapton HN substrate before and after a bend testing. The GO ink and the Ag ink were deposited using 60 and 5 inkjet passes, respectively. A), B) Optical images of the sensor before (A) and after (B) the bend testing. C) SE images with low and high (inset) magnification of a silver IDE of the sensor after the bend testing. D) SE image of the rGO patch of the sensor after the bend testing.

resistance between the two silver electrodes was 6 kΩ. Due to the factor that the most important advantages of the inkjet-printing of electronic devices on Kapton are probably the flexibility and mechanical robustness provided by the Kapton relative to other rigid substrates, the influence of bending of the Kapton-supported, all-ink-jet-printed rGO/Ag sensor on the electronic behaviour of the sensor was examined. The single-layered, all-inkjet-printed gas sensor shown in Fig. 5A was bent to a radius of curvature of ~1 cm 1,000 times in tension and anther 1,000 times in compression. The conductivity of the sensors was measured after every 50 times of bending. It was found that the conductivity of the sensor virtually remained the same (i.e., ~6 kΩ) throughout the whole bend testing as that before the bending. After such repeated bending, morphology of the sensor was examined via optical and SEM microscopic analyses. As shown in Figs. 5B, 5C and 5D, no apparent cracks on either the rGO or the silver films were found.

### 3.6 Gas sensing with all-inkjet-printed flexible gas sensors

An all-inkjet-printed gas sensor fabricated on a 4-PEM-layer-modified Kapton HN film following the procedures illustrated in Fig. 4 was exposed to 2.0 ppm of diethyl ethylphosphonate (DEEP). Fig. 6 shows the sensing behaviour (relative sensitivity versus exposure time) of the sensor. The relative sensitivity S is defined by the formula

$$S = (R-R_0)/R$$

Where R is the resistance between the two silver electrodes of the sensor at a particular time after the sensor has been exposed to the DEEP vapor or nitrogen and $R_0$ that right before the exposure.

As shown in Fig. 6, the sensor was virtually non-responsive to the carrying gas nitrogen. The resistance of the sensor immediately began to increase upon the onset of 2.0 ppm DEEP and kept increasing during the duration of the DEEP release. A relative sensitivity of 1% was obtained after about 9 min of exposure to the 2.0 ppm DEEP. A relative sensitivity of 5.2% was reached after exposure to the DEEP vapor for 63 min (Fig. 6). It is worth mentioning that the proof-of-concept

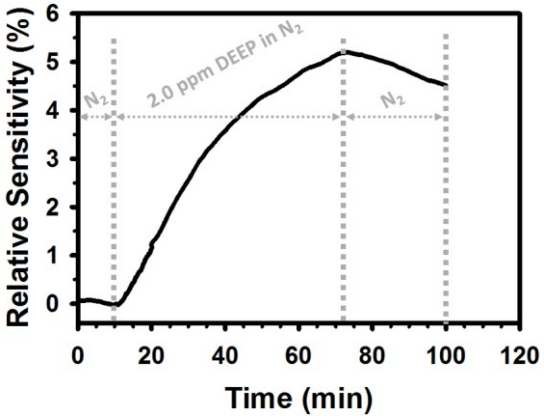


**Fig. 6.** Typical sensing behaviour of a fully-inkjet-printed rGO-based sensor upon exposure to 2.0 ppm DEEP.

sensor prototype inkjet-printed in this work used the intrinsic properties of rGO to sense DEEP and the sensing material was not optimized for the analyte. It has been reported that a hexafluoroisopropanol group-containing chemoselective compound (selector) was usually used to functionalize a sensing material to enhance its sensitivity to G-series nerve agent simulants including DEEP (the enhancement in sensitivity was due to the hydrogen bonding interaction between the selector and the simulants).[37-39] Since the surface modification approach reported in this work generally reduces the inherent surface hydrophobicity of Kapton HN films and allows for great wettability of both water- and organic solvent-based inkjet-inks, functionalization of the sensing materials should not affect the printability of the resulting sensing material inks on such surface modified substrates. As a matter of fact, work is underway in our group to fully inkjet-print flexible, lightweight and miniature-sized sensors on surface modified Kapton HN films either with inks made of functionalized sensing materials or by printing a thin film of a chemoselective compound on top of the inkjet-printed sensor material patches."

## 4. Conclusions

An automated, readily-scalable, layer-by-layer, PEM surface modification process has been developed to tune the Kapton HN surface properties to allow for the inkjet printing of both water-based and organic solvent-based inks with desired printability, thus facilitating the low-cost fabrication of flexible, single-layered or multi-layered all-inkjet-printed electronic devices. This surface modification process involved the use of only weak polyelectrolytes (to enable systematic and simple control of the PEMs formed via adjustment of the pH of the polyelectrolyte solutions) and utilized the positive charges present on the Kapton HN due to the presence of Ca-bearing particles. Aqueous GO suspensions could be inkjet-printed into uniform films with desired patterns and sharp features on the modified Kapton HN substrates. Such patterned uniform films were retained upon drying (i.e., the coffee-ring effect was avoided), presumably due to the reduction in fluid motion during drying resulting from the local electrostatic interactions between the positively-charged PEM-modified Kapton HN surface and the negatively-charged GO flakes. Inkjet-printed GO films deposited on Kapton HN substrates modified with 4 PEM layers were found to be sufficiently robust as to survive post-printing drying, dry thermal reduction or liquid pyrrole-based reduction, and GO film chemical functionalization processes.

A single-layered, all-inkjet-printed rGO/Ag gas sensor fabricated on a 4-PEM-layer-modified Kapton HN substrate was resistant to repeated bending (1,000 times in tension and another 1,000 times in compression) to a 1 cm radius, as revealed by the retention of the electrical conductivity of the sensor and the apparent absence of cracks in the rGO and Ag films after such bending. While not optimized (such as

functionalized with a chemoselective compound) to sense a particular analyte, our proof-of-concept fully-inkjet-printed sensors showed a decent response to 2.0 ppm diethyl ethylphosphonate (DEEP, a G-series nerve agent simulant).

## Acknowledgements

This research was supported by the Defense Threat Reduction Agency via Award No. HDTRA1-09-14-FRCWMD/TA3. The work of KHS was also supported by Award No. FA9550-10-1-0555 (Air Force BIO-PAINTS MURI).

## Notes and references

1 I. Ota, J. Ohnishi and Yoshiyam.M, *Proc. IEEE*, 1973, **61**, 832-836.
2 G. H. Gelinck, H. E. A. Huitema, E. Van Veenendaal, E. Cantatore, L. Schrijnemakers, J. Van der Putten, T. C. T. Geuns, M. Beenhakkers, J. B. Giesbers, B. H. Huisman, E. J. Meijer, E. M. Benito, F. J. Touwslager, A. W. Marsman, B. J. E. Van Rens and D. M. De Leeuw, *Nat. Mater.*, 2004, **3**, 106-110.
3 L. S. Zhou, A. Wanga, S. C. Wu, J. Sun, S. Park and T. N. Jackson, *Appl. Phys. Lett.*, 2006, **88**.
4 T. Sekitani, T. Yokota, U. Zschieschang, H. Klauk, S. Bauer, K. Takeuchi, M. Takamiya, T. Sakurai and T. Someya, *Science*, 2009, **326**, 1516-1519.
5 T. R. Le, V. Lakafosis, M. M. Tentzeris, Z. Y. Lin, Y. N. Fang, K. H. Sandhage and C. P. Wong, Nuremberg, Germany, 2013.
6 J. D. Shi, X. M. Li, H. Y. Cheng, Z. J. Liu, L. Y. Zhao, T. T. Yang, Z. H. Dai, Z. G. Cheng, E. Z. Shi, L. Yang, Z. Zhang, A. Y. Cao, H. W. Zhu and Y. Fang, *Adv. Funct. Mater.*, 2016, **26**, 2078-2084.
7 C. G. Granqvist, *Sol. Energy Mater. Sol. Cells*, 2007, **91**, 1529-1598.
8 J. Yoon, A. J. Baca, S. I. Park, P. Elvikis, J. B. Geddes, L. F. Li, R. H. Kim, J. L. Xiao, S. D. Wang, T. H. Kim, M. J. Motala, B. Y. Ahn, E. B. Duoss, J. A. Lewis, R. G. Nuzzo, P. M. Ferreira, Y. G. Huang, A. Rockett and J. A. Rogers, *Nat. Mater.*, 2008, **7**, 907-915.
9 B. Schmied, J. Gunther, C. Klatt, H. Kober and E. Raemaekers, *Smart textiles*, Trans Tech Publications Ltd, Stafa-Zurich, Switzerland, 2009.
10 T. H. Han, Y. Lee, M. R. Choi, S. H. Woo, S. H. Bae, B. H. Hong, J. H. Ahn and T. W. Lee, *Nat. Photonics*, 2012, **6**, 105-110.
11 M. X. Chen, *Proc. IEEE*, 2005, **93**, 1339-1347.
12 K. Myny, S. Steudel, P. Vicca, M. J. Beenhakkers, N. van Aerle, G. H. Gelinck, J. Genoe, W. Dehaene and P. Heremans, *Solid State Electron.*, 2009, **53**, 1220-1226.
13 H. Sirringhaus, T. Kawase, R. H. Friend, T. Shimoda, M. Inbasekaran, W. Wu and E. P. Woo, *Science*, 2000, **290**, 2123-2126.
14 T. Shimoda, K. Morii, S. Seki and H. Kiguchi, *MRS Bull.*, 2003, **28**, 821-827.
15 T. R. Hebner and J. C. Sturm, *Appl. Phys. Lett.* , 1998, **73**, 1775-1777.
16 S. Jung, A. Sou, K. Banger, D. H. Ko, P. C. Y. Chow, C. R. McNeill and H. Sirringhaus, *Adv. Energy Mater.*, 2014, **4**.
17 T. R. Le, V. Lakafosis, Z. Y. Lin, C. P. Wong and M. M. Tentzeris, San Diego, CA, USA, 2012.
18 I. Gouzman, O. Girshevitz, E. Grossman, N. Eliaz and C. N. Sukenik, *ACS Appl. Mater. Inter.*, 2010, **2**, 1835-1843.
19 N. Inagaki, S. Tasaka and K. Hibi, *J. Polym. Sci. Pol. Chem.* , 1992, **30**, 1425-1431.
20 B. J. Bachman and M. J. Vasile, *J. Vac. Sci. Technol. A*, 1989, **7**, 2709-2716.
21 J. W. Shin, J. P. Jeun and P. H. Kang, *Macromol. Res.*, 2010, **18**, 227-232.
22 I. Ghosh, J. Konar and A. K. Bhowmick, *J. Adhes. Sci. Technol.* , 1997, **11**, 877-893.
23 X. D. Huang, S. M. Bhangale, P. M. Moran, N. L. Yakovlev and J. S. Pan, *Polym. Int.* , 2003, **52**, 1064-1069.
24 R. R. Thomas, S. L. Buchwalter, L. P. Buchwalter and T. H. Chao, *Macromolecules*, 1992, **25**, 4559-4568.
25 Y. J. Park, D. M. Yu, J. H. Ahn, J. H. Choi and Y. T. Hong, *Macromol. Res.*, 2012, **20**, 168-173.
26 B. T. Least and D. A. Willis, *Appl. Surf. Sci.*, 2013, **273**, 1-11.
27 L. Gallais, E. Bergeret, B. Wang, M. Guerin and E. Benevent, *Appl. Phys. A-Mater.*, 2014, **115**, 177-188.
28 X. D. Guo, Y. Dai, M. Gong, Y. G. Qu and L. E. Helseth, *Appl. Surf. Sci.*, 2015, **349**, 952-956.
29 D. Yoo, S. S. Shiratori and M. F. Rubner, *Macromolecules*, 1998, **31**, 4309-4318.
30 P. S. Wang, T. N. Wittberg and J. D. Wolf, *J. Mater. Sci.*, 1988, **23**, 3987-3991.
31 E. B. Secor, P. L. Prabhumirashi, K. Puntambekar, M. L. Geier and M. C. Hersam, *J. Phys. Chem. Lett.*, 2013, **4**, 1347-1351.
32 C. A. Amarnath, C. E. Hong, N. H. Kim, B. C. Ku, T. Kuila and J. H. Lee, *Carbon*, 2011, **49**, 3497-3502.
33 K. Lowack and C. A. Helm, *Macromolecules*, 1998, **31**, 823-833.
34 M. K. Williams, A. E. Smith, M. A. Huelskamp, K. P. Armstrong, J. L. Brandon and J. M. Lavoie, *Kapton HN Investigations*, MOUND, 1990.
35 P. Somasundaran and G. E. Agar, *J. Colloid Interf. Sci.*, 1967, **24**, 433-440.
36 Z. P. Li, J. Q. Wang, Z. F. Wang, H. Q. Ran, Y. Li, X. X. Han and S. R. Yang, *New J. Chem.*, 2012, **36**, 1490-1495.
37 K. A. Mirica, J. M. Azzarelli, J. G. Weis, J. M. Schnorr and T. M. Swager, *Proc. Natl. Acad. Sci. USA.*, 2013, **110**, E3265-E3270.
38 E. S. Snow, F. K. Perkins, E. J. Houser, S. C. Badescu and T. L. Reinecke, *Science*, 2005, **307**, 1942-1945.
39 L. T. Kong, J. Wang, X. C. Fu, Y. Zhong, F. L. Meng, T. Luo and J. H. Liu, *Carbon*, 2010, **48**, 1262-1270.

View Article Online
DOI: 10.1039/C6TC01066K

Kapton HN films were surface modified, for the first time, by taking advantage of their additive and using only weak polyelectrolytes, for all-inkjet-printed flexible electronic devices.